

Article

A Unique Crustacean-Based Chitin Platform to Reduce Self-Aggregation of Polysaccharide Nanofibers

Carolina Londoño-Zuluaga ¹, Hasan Jameel ¹, Ronalds Gonzalez ¹, Kimberly Nellenbach ², Ashley Brown ², Guihua Yang ^{3,*} and Lucian Lucia ^{1,2,3,4,*}

¹ Department of Forest Biomaterials, North Carolina State University, Raleigh, NC 27695-8005, USA

² Joint Department of Biomedical Engineering, North Carolina State University, Raleigh, NC 27695-8005, USA

³ State Key Laboratory of Biobased Materials & Green Papermaking, Qilu University of Technology/Shandong Academy of Sciences, Jinan 250353, China

⁴ Department of Chemistry, North Carolina State University, Raleigh, NC 27695-8204, USA

* Correspondence: ygh2626@126.com (G.Y.); lalucia@ncsu.edu (L.L.)

Abstract: Every year, over 8 million tons of crustacean shells are discarded. However, there exists an opportunity for valorizing the chitin and calcium carbonate part of the composition of the shells. Our study revealed crustacean chitin reduces self-aggregation effects. It was shown that crustacean-based nanofibers alone or added to cellulose offer unprecedented reductions in viscosity even after drying to produce foams impossible for cellulose. Polysaccharide nanofibers suffer from increased viscosity from strong hydrogen bonding addressed by the incorporation of crustacean-based nanofibers. The ability of the nanocomposite to overcome self-aggregation and collapse was attributed to organized chitin nanofiber morphology in the crustacean matrix. As a result of enhanced surface area from reduced fiber aggregation, the chitin/crustacean-cellulose blend was tested for a biomedical application requiring a high surface area: coagulation. Preliminary experiments showed the crustacean matrices, especially those containing calcium carbonate, induced blood clotting when 35 s. A materials platform is proposed for bio-based nanofiber production overcoming intractable and difficult-to-address self-aggregation effects associated with polysaccharides.

Keywords: polysaccharide nanofibers; crustacean shells; chitin; cellulose; self-aggregation; clotting; foams



Citation: Londoño-Zuluaga, C.; Jameel, H.; Gonzalez, R.; Nellenbach, K.; Brown, A.; Yang, G.; Lucia, L. A Unique Crustacean-Based Chitin Platform to Reduce Self-Aggregation of Polysaccharide Nanofibers. *Fibers* **2022**, *10*, 87. <https://doi.org/10.3390/fib10100087>

Academic Editors: Ionela Andreea Neacsu and Alexandru Mihai Grumezescu

Received: 28 July 2022

Accepted: 11 October 2022

Published: 14 October 2022

Publisher's Note: MDPI stays neutral with regard to jurisdictional claims in published maps and institutional affiliations.



Copyright: © 2022 by the authors. Licensee MDPI, Basel, Switzerland. This article is an open access article distributed under the terms and conditions of the Creative Commons Attribution (CC BY) license (<https://creativecommons.org/licenses/by/4.0/>).

1. Introduction

Nanofibers sourced from natural feedstocks have been drawing attention in the chemistry, physics, materials, and engineering research community for their unprecedented properties from their non-linearized nanoscopic dimensions [1–4]. For example, they have been found to significantly improve mechanical strengths, endow non-linear optics, and provide very high surface area compared to their bulk analogues.

Biologically derived nanofibers have enhanced the scope of applications commensurate or superior to their synthetic analogues such as witnessed in tissue engineering [5], paper electronics [6], and packaging [7]. Because of their abundance, biocompatibility, renewability, biodegradability, and fundamentally appealing nanoscopic building block nature, cellulose and chitin are among the most versatile materials for nanofiber production [8].

Chitin and its deacetylated derivative chitosan are cellulose analogues which possess the classical motif of anhydroglucopyranose units bonded by β -1-4 linkages. Chitin displays N-acetyl units at the C2 position thus distinguishing it from cellulose, whilst chitosan is mostly deacetylated chitin (>72%). Although chitin is a semi-crystalline and valuable biopolymer, most seafood-based shells are not exploited for any downstream applications [8].

It is estimated that > 8 million tonnes per year of crustaceans produced by the seafood industry are therefore wasted. This valuable resource, however, has great potential to be

valorised for a host of materials and engineering applications based on their nanofibers [9]. However, although chitin and chitosan can be made into nanofibers, low yields, and complicated chemical treatments lead to unnecessary expenses. Yet, it is known that chitin after chemical modification can fetch > 17,000 USD/ton as of recently [10].

The preparation of chitin nanofibers requires chitin extraction. Common methods include chemical extraction by alkali and acid [11], enzymes [12], and non-chemical treatments using hot water and carbonic acid [13]. However, these methods, including reduction of molecular weight and degree of acetylation [14], adversely impact nanofiber formation and incur expense.

Today, chitin nanofibers are commonly produced by electrospinning or mechanical treatments. Chitin is not easily electro-spun due to solubility limitations in most common organic solvents. γ -radiation is one means to partially depolymerize it and encourage solvation [15] although this approach compromises final mechanical integrity. A common deacetylation degree is ~8% for chitin in electrospinning [16] for which typical solvents are mixtures of N, N-dimethylacetamide (DMAC) with lithium chloride (LiCl), 1,1,1,3,3,3-hexafluoro-2-propanol (HFIP), a mixture of sodium hydroxide with urea, and different mixtures of ionic liquids [15].

In mechanical grinding, a slurry of isolated chitin (~1%) [8] in water is passed through either a Masuko grinder, a dynamic high-pressure homogenizer, or a high-pressure water jet system [15]. However, chitin drying following extraction leads to hydrogen bonding among hydroxyl groups, acetamide, and amino groups leading to intractable aggregation effects which make it very difficult to further process [17]; in fact, the viscosity of the resulting systems is so high and displays such a high resistance to dispersion in solutions that it nearly abrogates any possibility of future applications. It is therefore incumbent on any product design to overcome interfibrillar hydrogen bonding for successful application of chitin and its derivatives [15].

To date, the manufacture of dispersible nanofibers from crustacean shells has little to no precedent. Any successful application must overcome viscosity effects without significant modifications or chemical treatments; we have therefore developed an ingenious method which involves using crustacean-based nanochitin to overcome increased viscosity effects generally observed in non-crustacean-based chitin nanofibers.

Previous work in production of chitin/cellulose nanocomposites directly employed isolated chitin and required pre-treatments before the isolation of CNF to successfully make non-aggregated composites. For instance, Hassan, Hassan, and Oksman [18] demonstrated alkali or xylanase enzyme treated CNF/chitosan films have much greater wet and dry tensile strength than their untreated analogues. Azeredo et al. [19] optimized CNF/chitosan films by a casting technique that required glycerol to properly homogenize the system and its casting ability.

By increasing availability to chitin functional groups, i.e., generating a more open structure, numerous applications can be pursued. It is known that chitin/chitosan systems have been implicated in the ability to cause blood cell aggregation [20] by virtue of their partially positive available amine groups interacting electrostatically with negatively charged thrombocytes and erythrocytes to induce clumping and thus aggregate formation [21,22]. Recently, high surface area chitosan-based dressings have been proposed to arrest bleeding without platelets and coagulation or clotting factors [23,24]. By affording a much more open chitin/chitosan structure, wound treatment (e.g., antimicrobial behavior, oxygen permeability) [25,26] is likely for catastrophic external hemorrhaging [27], surgery [28,29], and rural care [30].

Thus, the importance of the current work is found in the development of a nanofiber composite platform using the chitin in seafood waste for reducing self-aggregation effects typically associated with the production of nanoscopic polysaccharides. As mentioned, polysaccharide nanofibers have a very high propensity to self-aggregate due to very favourable inter/intra-hydrogen bonding effects. The intrinsic advantage of our system is that *the multi-component pre-existing non-entangled polysaccharide matrix of a crustacean shell*

overcomes aggregation effects within itself or after being mixed with another polysaccharide such as cellulose which is often highly susceptible to self-aggregation.

2. Materials and Methods

2.1. Materials

Crustacean shells were purchased from a seafood processing company, whereas sodium hydroxide pellets, hydrochloric acid 6N and acetic acid glacial (98%) were purchased from VWR.

2.2. Equipment

A super mass collider grinder, Masuko MKCA 6-5, was used with MKGA-C stone for nano-fibrillation. The Masuko series of friction grinding machines produce ultra-fine particles which have the appearance of paste. The super mass collider's ultra-fine grinders feature two ceramic nonporous grinders, which are adjustable to any clearance (typically it is negative) between the upper and lower grinders. Using ceramic grinders enables the production of particles that are rounder in morphology and smoother with a more uniform grain size than by any other crushing method.

2.3. Methods

Shell cleaning and particle size reduction. Crustacean shells were washed and cleaned using deionized water and oven dried at 60 °C for 4 h. Particle size reduction was performed using a standard Wiley Mill to provide 40 mesh particle size. Crustacean control materials are referred to as CSAM.

Crustacean shell component extraction. Component parts of the crustacean shells (mineral and organic parts) were isolated using successive alkali and acid treatments. For chitin (Ch) extraction from the 40-mesh crustacean shell, protein was removed using 1 M sodium hydroxide at 65 °C for 2 h [31]. The level of protein removal as revealed by XPS was ~100% (no detectable amide nitrogen signal vs. chitosan amine signal, 399.9 eV vs. 399.1 eV, respectively) to produce Non-Protein Crustacean Shell (NPCS). Subsequently, calcium carbonate and minerals were removed by soaking in hydrochloric acid 1.5 M at room temperature for 5 h [32] to produce NCCS (Non-Calcium Carbonate Crustacean Shell). The level of removal of Ca removal was ~100% as revealed by XPS. NPCS samples and NCCS samples were therefore produced by removing protein and minerals, respectively, through successive alkali and acid treatments.

Crustacean shell-based slurry preparation and grinding. Crustacean shell samples for future chemical processing were first ground to a 40-mesh slurry in tap water at a solids content of 3%. Next, a 1% solution was made [33] in which the solution pH was kept at 3 by adding acetic acid [8]. Once the solution was prepared, the slurry was ground using the Masuko at 2000 rpm with a variable gap width. Finally, the slurry was freeze-dried and characterized as shown in the following section.

2.4. Characterization

Fourier transform infrared spectroscopy (FT-IR). The analysis of functional groups present was done using a Perkin-Elmer Frontier IR single range spectrometer. The spectral window for the analysis was 4000–650 cm^{-1} at a resolution of 4 cm^{-1} over 32 scans.

X-Ray Diffraction (XRD). Rigaku Smart Lab X-Ray diffractometer was used for XRD measurements of powdered samples. The data were obtained at 2θ within a scanning range between 5 and 40° [11]. Crystallinity was determined by the area under the curve of the peaks associated with each of the components.

Scanning electron microscopy (SEM). Morphological analysis of the samples was done by SEM using the Field Emission Scanning Electron Microscope FEI Verios 460L. The samples were covered with a 7 nm layer of gold. The voltage was between 1.00 and 2.00 kV, whilst a 13 pA current was used. For higher magnification, 500 V bias was used to reduce sample charging.

X-ray photoelectron spectroscopy (XPS). The XPS study was carried out using a Kratos Axis Ultra DLD X-ray Photoelectron Spectrometer equipped with a graphite monochromator and Al K α radiation.

Crustacean Based Nanofibers. Two very important fiber applications were considered: nanofibers and crustacean shell composites with cellulosic pulps. For crustacean shell-based nanofibers, Non-Protein Crustacean Shell (NPCS), Non-Calcium Carbonate Crustacean Shell (NCCS), and Chitin (Ch) were evaluated as blood clotting materials by employing hemostatic assays followed by confocal microscopy.

Hemostatic Assay, Rapid Clot test. 50 μ L fibrin clots (2.5 mg/mL fibrinogen) were generated in the presence or absence of 0.25 μ /mL thrombin in tubes. Clotting was visually observed over 10 min [34].

Confocal microscopy. 50 μ L fibrin clots (2.5 mg/mL fibrinogen) were formed in the presence or absence of 0.25 μ /mL thrombin with Alexa 488 labeled fibrinogen for visualization. Clots were formed with 10% total volume NCCS, NPCS and Ch particles. Clots were polymerized for 3 h prior to imaging.

Crustacean shell co-grinding with cellulosic pulp. A slurry was prepared at 3% total solid contents with different ratios of Crustacean Shell: Northern Bleached Softwood Kraft (NBSK) Pulp Cellulose (10:90, 20:80, 30:70). The mixtures were passed through the Masuko grinder at 2000 rpm and variable gap width. The final slurry was freeze-dried and characterized. The number of passes was decided after performing preliminary tests. In preliminary tests, the power needed to operate the Masuko was also used as a parameter to determine what would be the optimum number of passes. A higher power output was an indication of material stuck between the rocks and inefficient grinding

3. Results and Discussion

3.1. Material Characterization

Crustacean shell-based nanofibers were produced by the Masuko grinder in which the final slurry was freeze-dried for characterization. FT-IR was used before and after mechanical treatment to identify changes in the molecular framework, specifically, identifying key functional groups and extent mechanical treatment/particle size reduction induces chemical changes. For minerals, it is known that particle size reduction can shift functional groups to lower wavenumbers [35]. However, in crustacean shells containing calcium carbonate, previously identified as calcite, the calcium carbonate peaks showed an increase in intensity, but no shifts.

With respect to the peaks associated with chitin, no differences were observed. Unlike previous findings, grinding did not affect the absorbance of individual particles and the overall structure [36]. It is likely that the mechanochemical energy over the time frame for grinding expended in our situation was not sufficient to induce chemical changes. The surface area was the only parameter that changed. In the crustacean shells, bands at wavenumbers 3262, 1635, 1402, 1052 and 872 cm^{-1} were observed and, respectively, attributed to NH stretching, -N-, H-CO stretching, NH₂ groups in protein, and calcium carbonate [37,38]. Figure 1 supports the lack of shift changes in peaks but suggests an increase in functional group availability.

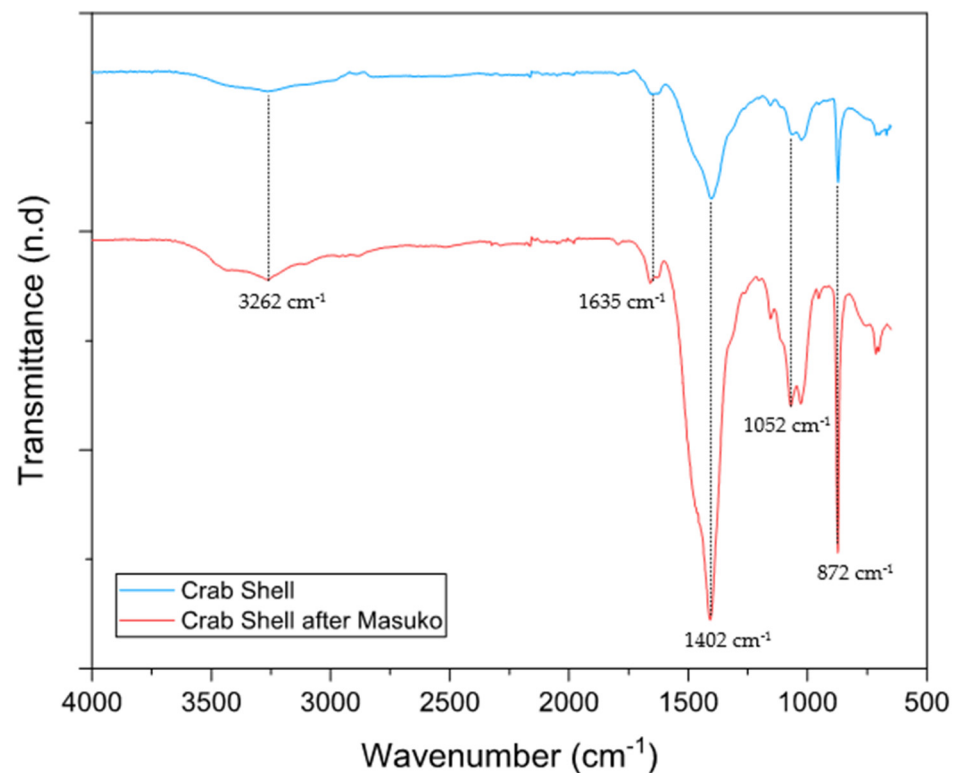


Figure 1. FTIR spectra of virgin crab shell and crab shell after grinding using Masuko Grinder. Wavenumbers at 3262, 1635, 1402, 1052 and 872 cm^{-1} are attributed to NH stretching, -N- , H-CO stretching, NH_2 groups in protein, and calcium carbonate [37,38].

X-Ray Diffraction was performed to determine the effects of mechanical grinding on the crystallinity of calcium carbonate (calcite) and chitin. As shown in Figure 2, incremental changes in chitin were observed when the number of passes and energy increased. In general, chitin is a linear semi-crystalline polymer with diffraction peaks at $2\theta \sim 9.24^\circ$, 12.90° , 19.18° , 23.36° , and 26.14° from the planes (020), (101), (110), (130), and (013), respectively [39,40]. In crustacean shells, the main peaks correspond to minerals which are present in a higher quantity such as calcium carbonate in the form of calcite.

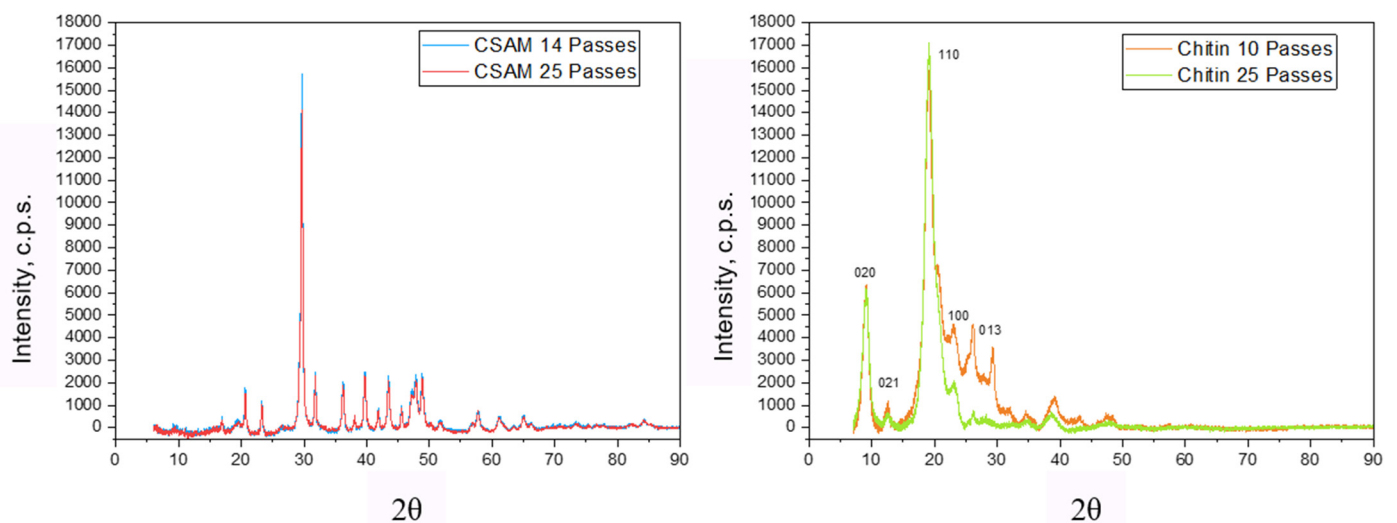


Figure 2. X-Ray diffraction patterns for crustacean shell (CSAM) and chitin after Masuko grinding over 14 and 25 grinding passes.

With respect to the effect of the energy/number of passes, in crustacean shells as manufactured (CSAM) a higher peak intensity ($>13\%$) was observed in the calcium carbonate peak (at $2\theta = 30^\circ$) when 14 grinding passes instead of 25 passes were applied, which indicates a higher degree of crystallinity due to higher order and increased molecular packing.

For chitin, peak intensity was also higher as fewer passes were used ($2\theta = 20\text{--}30^\circ$). For example, after 25 passes, several of the peak intensities for $2\theta = 30$ tended to decrease and almost disappeared, whilst a slight increase in the intensity of the peaks corresponding to planes (020) and (110) was observed. It thus cannot be concluded definitively that a steady state effect on crystallinity was obtained because various crystalline planes differed in magnitude. Work on the effect of ball mill grinding on chitin crystallinity [40,41], however, definitively showed a decrease, but that work was done under dry conditions; in the present case, water was used, which likely behaved as a plasticizer to partially maintain various planes of crystallinity. Figure 3 revealed that the passes did not help to de-aggregate the matrix.

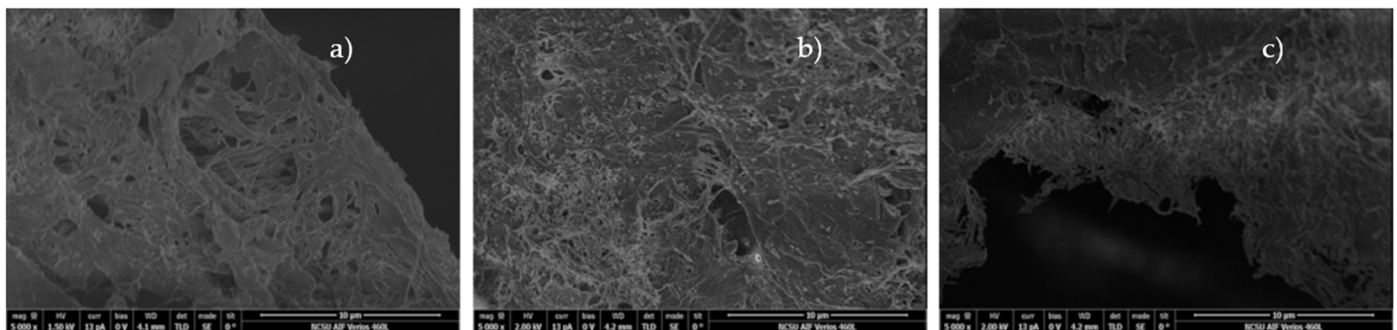


Figure 3. SEM images for chitin after Matsuko grinding (a) 5 passes, (b) 10 passes, (c) 25 passes. The scale bars at the lower right of the left, middle, and right micrographs correspond to $10\ \mu\text{m}$. Notice in all passes aggregation was pronounced (a more smooth texture in general).

After the wet grinding of all samples, we attempted to visually inspect the formation of nanofibers. Interestingly, it was found only for pure chitin samples (non-crustacean) that aggregates were formed; in other words, individualized nanofibers were NOT present. Remarkably, the grinding of crustacean shells greatly facilitated individualized nanofiber formation by lowering the activation barrier to the formation of the suspension and avoiding the extent of hydrogen bonding (self-adhesion effects), thus making them much easier to grind, a result which has not been previously observed and constitutes a chief finding of our study. The results elaborated above are validated using SEM as shown in Figures 3 and 4.

XPS analyses were pursued with the objective of determining the type of functional groups that were prevalent on the surface after grinding. Survey spectra were obtained in which Auger peaks corresponding to O 1s, C 1s and O were observed in all samples. For crustacean shell samples, calcium peaks are appreciably more apparent than in non-protein crustacean shell. Furthermore, crustacean shell samples showed peaks related to sodium and chlorite, which indicate contamination of salts from cleaning before grinding. In addition to the survey spectra, spectra for nitrogen, oxygen and calcium were obtained. A summary of those results is described in Table 1.

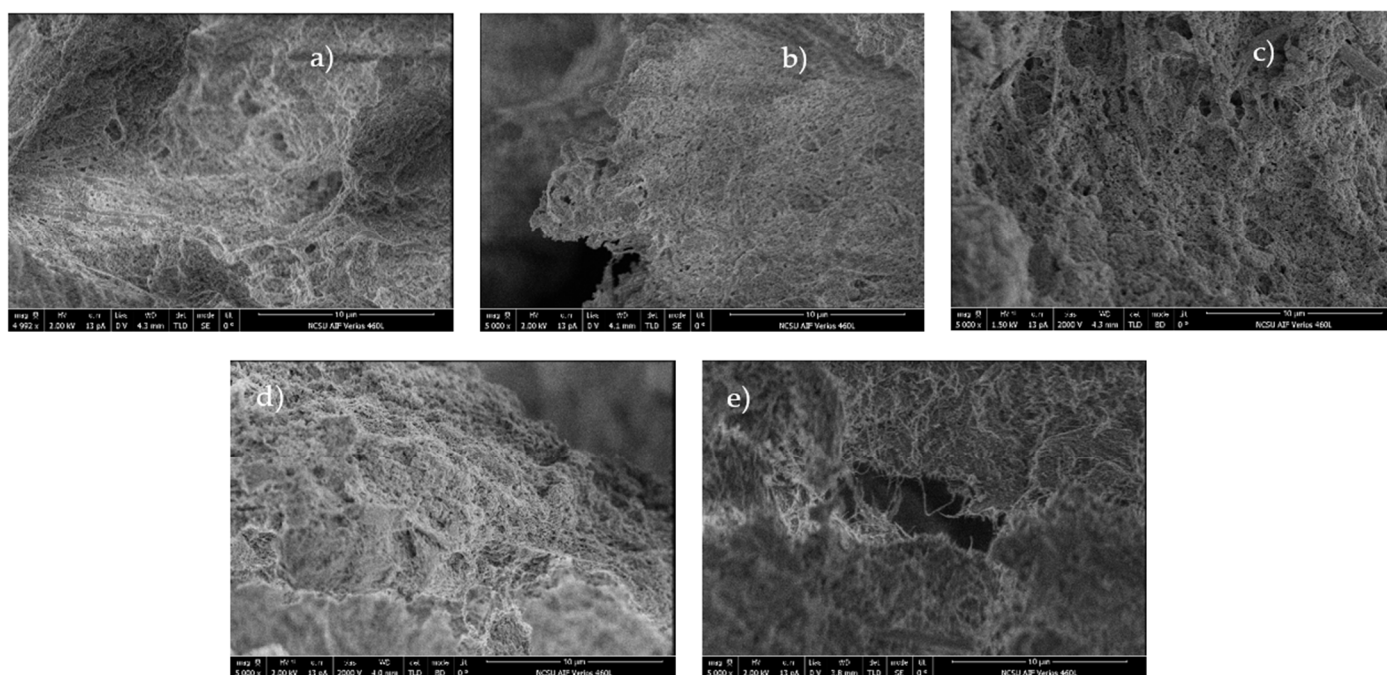


Figure 4. SEM images for non-protein crustacean shell after Matsuko grinding (a) 5 passes, (b) 10 passes, (c) 15 passes, (d) 20 passes, (e) 25 passes. The scale bars at the lower right of all five (5) micrographs correspond to 10 µm. Notice in consecutive passes a much more open (porous) structure suggesting reduced aggregation of fibrillar units.

Table 1. XPS results comparison of samples after various grinding passes.

Ratio	Chitin 25 ¹	NPCS 14 ²	CSAM 14 ³	CSAM 25 ⁴
C/O	2.58	1.54	1.42	1.29
C/N	12.45	38.05	12.64	11.46
C/Ca	400	7.36	8.35	8.70
O/N	4.82	24.75	8.88	8.82

¹ Chitin 25 = 25 passes, ² NPCS = Non-Protein Crustacean Shell 14 passes, ³ CSAM 14 = Crustacean Shell Control 14 passes, ⁴ CSAM 25 = Crustacean Shell Control 25 passes; all reported data within ± 0.05 standard deviation in a 95% confidence interval.

The results were obtained by determining the ratio of the areas under the curve for each element. In the case of chitin, because (calcium) is nearly zero, the ratio C/C_a is quite high. For crustacean shell samples, the differences between NPCS and CSAM are mainly due to the C/N and O/N ratios because the NPCS protein (source of N) was significantly reduced, hence significantly diminishing the denominator of the C/N ratio, whilst most other atoms remained the same. Thus, Table 1 in tandem with XPS data is supportive of the fact that targeting protein removal does not affect remaining calcium or chitin moieties to any great extent with very mild concomitant atom losses.

3.2. Crustacean Shell Co-Grinding with Cellulosic Pulp

One of the substantive issues of producing dispersible nanocellulose is the inability to avoid the strong hydrogen bonding formed within and among cellulose chains as predicated by hydrogen bonding effects leveraged by water. This problem SEVERELY limits nanocellulose dispersibility, thus restricting many applications. To overcome these technical challenges, pre-treatments had been applied to limit hydrogen bonding and repulsive charges, which have included enzyme treatment, acetylation, pulp refining, acid and alkali treatments and TEMPO (TEMPO: 2,2,6,6-Tetramethylpiperidin-1-yl)oxyl)-mediated oxidation [42].

At the industrial scale, calcium carbonate is used as a filler to avoid increased viscosity due to hydrogen bonding. Thus, a mixture of crustacean shells as made (CSAM) which has a high calcium carbonate content with Northern Bleached Softwood Kraft pulp (NBSK) was mechanically fibrillated using a Masuko grinder. A suspension of 3% solid content was prepared using different NBSK: CSAM ratios whose subsequent suspensions were freeze-dried.

The ability of nanocellulose to form foam materials is well known. However, one major drawback is avoiding structural collapse during water removal owing to capillary effects, thus limiting its scale up [42]. Studies have used delayed calcium-induced gelation, which by virtue of multivalent ion-induced aggregation of cellulose nanofibers, foam formation and increased strength can thus be favored [43].

Our preliminary results showed the formation of rigid, yet compression-resistant structures as shown in Figure 5. The samples were observed under SEM to show a gamut of fiber diameters, which indicates that not all cellulose fibers are yet on the nanoscale dimension, but many of them can be observed after reductions in particle size.

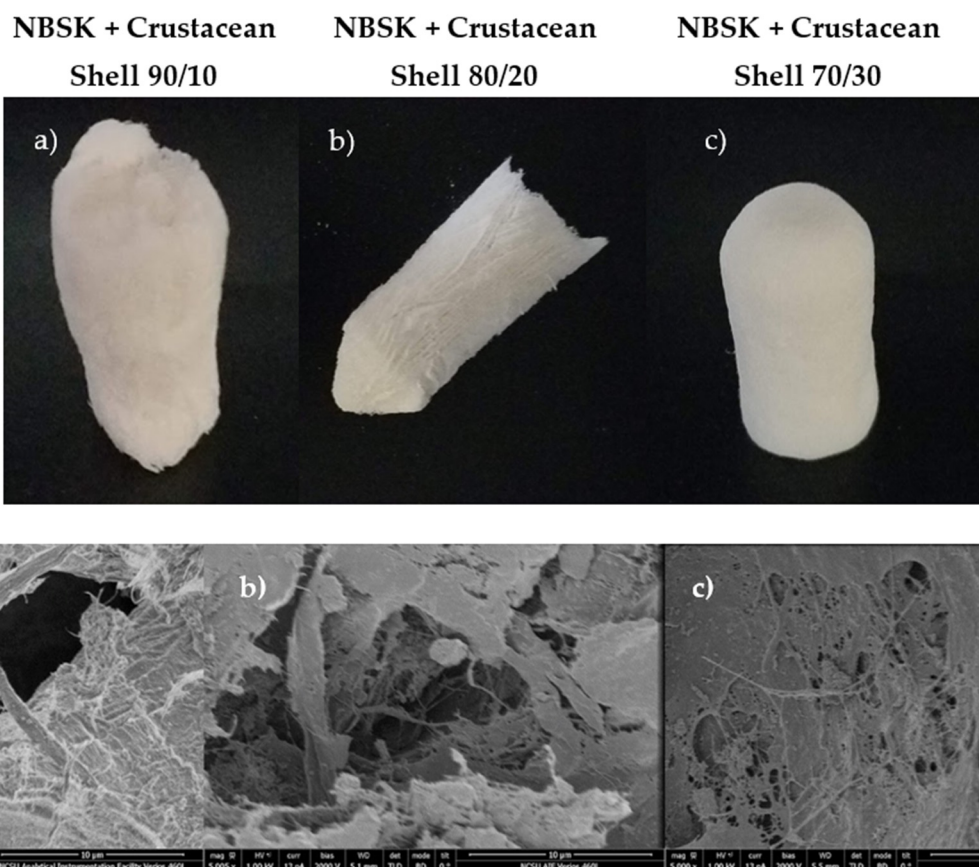


Figure 5. Cellulose-crustacean shell foams (a–c) represent gross (top) images and respective microscopic zooms (bottom): (a) NBSK+Crustacean Shell, 90/10, (b) NBSK+Crustacean Shell, 80/20, (c) NBSK+Crustacean Shell, 70/30, and accompanying SEMs (10-micron bar scale) formed by material co-grinding shown above followed by their respective SEM photomicrographs below the three images. Note the open porous structures which demonstrate the lack of fiber collapse.

Traces of nitrogen and calcium can be seen on the surface of the composites (Figure 6) whose peaks are not as intense as pure crustacean shell samples, but the presence of the two elements is indicative of chitin/protein and calcium carbonate likely distributed uniformly throughout the matrix that likely reduced the activation barrier to hydrogen bonding, self-aggregation, and capillary force-induced collapse. In the C spectra, peaks associated with CO_3^{-2} show very low intensity mainly due to a predominance of cellulose in the mixture

in which C–O peaks are sharper and thinner. Thus, we were able to fabricate foam-like structures that do not exhibit self-aggregation and are therefore in a similar manner NOT susceptible to the collapse behavior shown in many polysaccharides foam-based structures.

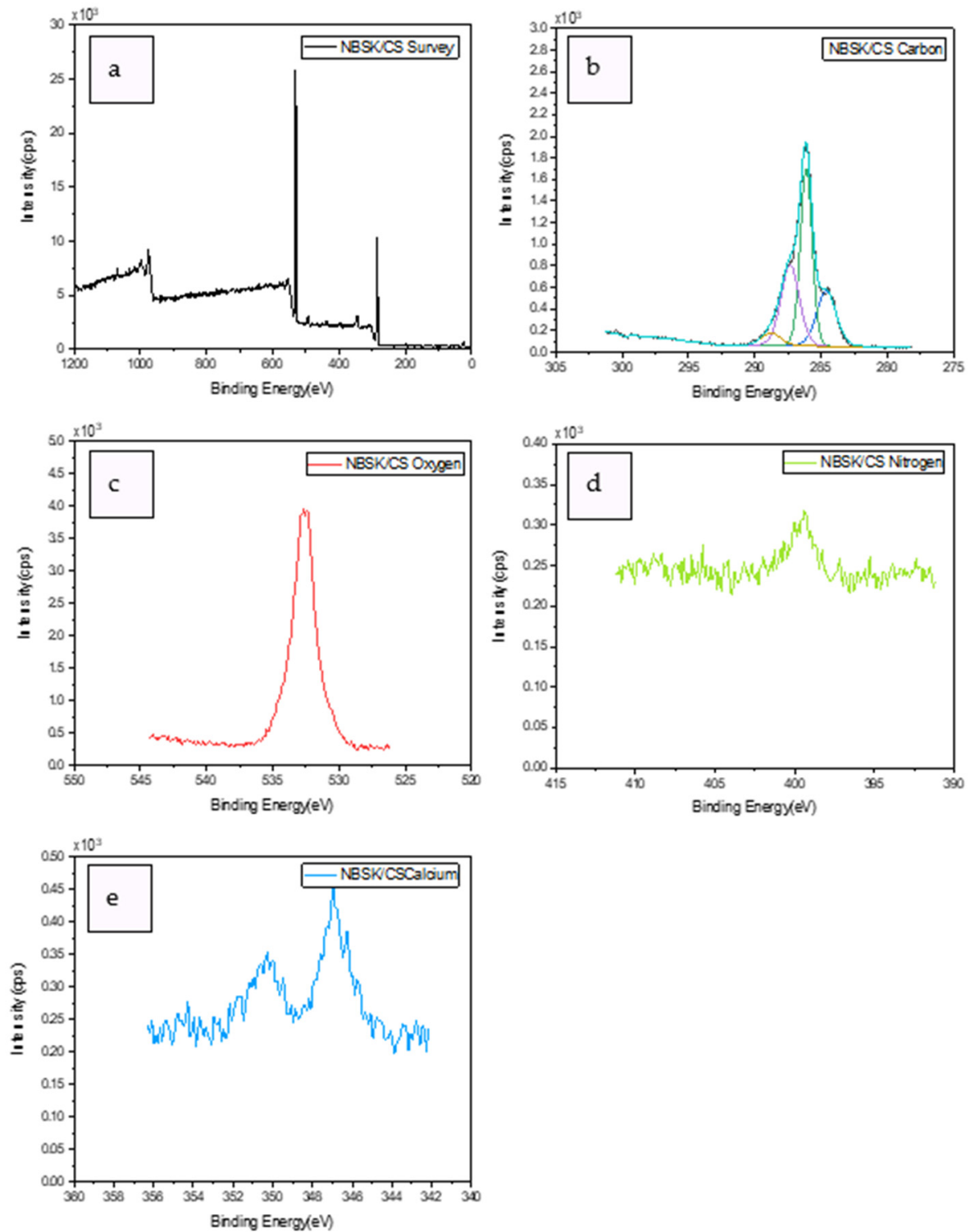


Figure 6. XPS Spectra for NBSK/CS 70:30: (a) full field survey, (b) carbon, (c) oxygen, (d) nitrogen, and (e) calcium.

3.3. Crustacean-Based Nanofiber Applications

Blood Clotting

To further investigate the significantly reduced self-aggregation supported by the crustacean-based polysaccharides, we opted to explore a very key biomedical application, clotting, in which surface area effects are paramount. In other words, affording optimal access to functional groups necessary for inducing clotting is key. Facile induction of blood clotting safely and efficiently has been widely studied because of its need for military operations, surgical procedures, and wound dressings. Today, the materials used for this purpose vary from inorganic to organic compounds as well as synthetic and natural polymers [44]. However, to date, no system has employed modified crustacean shell materials.

Blood clotting has two hemostatic pathways: a protein-based system and a platelet cascade-based system. In this case, it was decided to focus on a protein-based system that ends in the conversion of fibrinogen to fibrin, leading to the formation of thrombi [45]. To induce clotting via a protein-based system, ampholytic mucoprotein negative charges bond with positively charged groups [46]. Chitin and chitosan have been studied as suitable options due to the cationic nature presented by the amine group [44] as elaborated in the introduction. In general, it has been established that not all forms of chitin or chitosan are suitable for blood clotting because the hemostatic properties of these biopolymers are dependent on the degree of acetylation, molecular weight, and crystallinity [44].

Alternatively, calcium has been proven to induce a lower time for blood clot initiation, after which the presence of calcium in the blood increases the coagulation index [47] which has been associated with a higher clot strength [48]. Thus, pure chitin, non-protein crustacean shell, and non-calcium carbonate crustacean shell were used in hemostatic tests to determine the efficiency of these materials for blood clotting. In the case of chitin particles, it did not appear it induced clotting within an acceptable period in the absence of thrombin. In addition, their presence did not appear to hinder fibrin clot formation in the presence of thrombin. In Table 2, pure chitin seems to be the most efficient because it forms clots faster than other materials with thrombin.

Table 2. Hemostatic Essay Results.

Condition	Time to Clotting (Seconds)
Control:PPP, no thrombin	No clotting observed
Control:PPP, + thrombin	36 s
Ch 1%: PPP, no thrombin	No clotting observed
Ch 1%: PPP, + thrombin	15 s
¹ NCCS:PPP, no thrombin	No clotting observed
¹ NCCS:PPP, + thrombin	30 s
² NPCS: PPP, no thrombin	No clotting observed
² NPCS:PPP, + thrombin	35 s

¹ NCCS = Non-Calcium Carbonate Crustacean Shell, ² NPCS = Non-Protein Crustacean Shell.

From observations with confocal microscopy, pure chitin nanoparticles induce a degree of blood clotting. From Figure 7, in the sample containing calcium carbonate, it was found that the clotting-induced mechanism was absent because no network formation was observed. Finally, for non-protein crustacean shells, acceptable network formation is observed mainly due to the presence of calcium carbonate in the matrix. In addition to what was stated previously, the possible formation of calcium salts is contributing to clotting. Furthermore, when in solution, calcium ions can interact with negative charges on the proteins present in the blood [49].

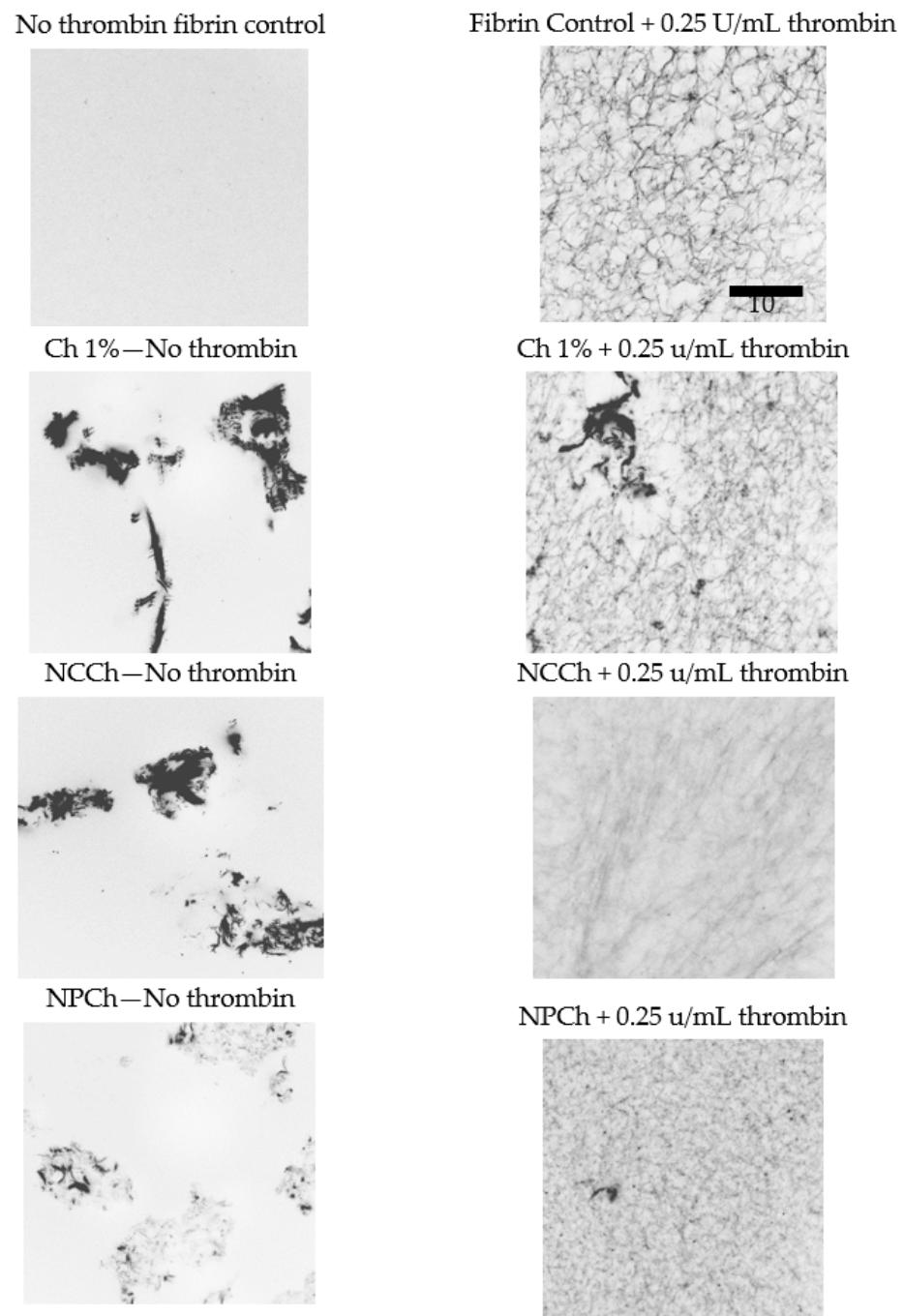


Figure 7. Confocal microscopy for blood clotting analysis for Chitin (Ch), Non-Calcium carbonate crustacean shell (NCCS) and Non-protein crustacean shell (NPCS).

4. Conclusions

Crustacean shell-based nanofibers can be efficiently produced by mechanical treatment of crustacean shells through Masuko grinding. **Our work has shown that crustacean shells by themselves or in combination with cellulosic pulp in a Masuko grinder without any prior pretreatments or chemistry overcome self-aggregation.** A novel platform was therefore discovered in this work for bio-based nanofiber production that overcomes previous self-adhesion/densification to thus leverage a significant green chemistry advantage. As a co-component with cellulose and calcium carbonate, a reduction was observed in solution viscosity due to attenuated hydrogen bonding, which during drying, afforded foam-like materials. Finally, with respect to blood clotting, the non-protein crustacean shell

provided an acceptable clot network formation mainly due to the presence of the calcium carbonate in the matrix which not participated in affording a higher surface/less that did not collapse but has already been proven to induce a lower time for blood clot initiation by increasing coagulation index which has been associated with a higher clot strength. In sum, the matrix of chitin-calcium carbonate and chitin-protein opens a wide range of possibilities for nanocomposites.

Author Contributions: Conceptualization, C.L.-Z. and L.L.; methodology, C.L.-Z.; validation, G.Y., R.G. and H.J.; formal analysis, C.L.-Z., L.L. and G.Y.; investigation, K.N. and A.B.; data curation, K.N. and A.B.; writing—original draft preparation, C.L.-Z. and L.L.; writing—review and editing, L.L., A.B. and G.Y.; supervision, L.L., R.G., H.J., G.Y. and A.B.; project administration, L.L.; funding acquisition, L.L., R.G., H.J. All authors have read and agreed to the published version of the manuscript.

Funding: The authors are grateful for the financial support from the Provincial Key Research and Development Program of Shandong (Grant No. 2021CXGC010601, 2019JZZY010326) and Pilot Project for Integrating Science, Education and Industry (2022JBZ01-05).

Data Availability Statement: Not applicable.

Acknowledgments: This work was performed in part at the Analytical Instrumentation Facility (AIF) at North Carolina State University, which is supported by the State of North Carolina and the National Science Foundation (award number ECCS-1542015). The AIF is a member of the North Carolina Research Triangle Nanotechnology Network (RTNN), a site in the National Nanotechnology Coordinated Infrastructure (NNCI). This work was also performed in part at Chapel Hill Analytical and Nanofabrication Laboratory, CHANL, a member of the North Carolina Research Triangle Nanotechnology Network, RTNN, which is supported by the National Science Foundation, Grant ECCS-1542015, as part of the National Nanotechnology Coordinated Infrastructure, NNCI. Confocal Microscopy and rapid clot tests were performed at the Advanced Wound Healing Lab.

Conflicts of Interest: The authors declare no conflict of interest. The funders had no role in the design of the study; in the collection, analyses, or interpretation of data; in the writing of the manuscript; or in the decision to publish the results.

References

1. Qin, J.; Zhao, J.; Wu, Y.; Li, L.; Li, D.; Deng, H.; Liu, J.; Zhang, L. Chitosan/collagen LBL-deposited nanofibers for improving the esophageal regeneration ability of nanofibrous mats. *Carbohydr. Polym.* **2022**, *286*, 119269. [[CrossRef](#)] [[PubMed](#)]
2. Zhang, G.; Chen, X.; Xu, W.; Yao, W.; Shi, Y. Piezoelectric property of PZT nanofibers characterized by resonant piezo-force microscopy. *AIP Adv.* **2022**, *12*, 035203. [[CrossRef](#)]
3. Park, J.; Jo, S.; Kim, Y.; Zaman, S.; Kim, D. Electrospun nanofiber covered polystyrene micro-nano hybrid structures for triboelectric nanogenerator and supercapacitor. *Micromachines* **2022**, *13*, 380. [[CrossRef](#)] [[PubMed](#)]
4. Ieamviteevanich, P.; Daneshvar, E.; Eshaq, G.; Puro, L.; Mongkolthananaruk, W.; Pinitsoontorn, S.; Bhatnagar, A. Synthesis and characterization of a magnetic carbon nanofiber derived from bacterial cellulose for the removal of diclofenac from water. *ACS Omega* **2022**, *7*, 7572–7584. [[CrossRef](#)]
5. Vasita, R.; Katti, D.S. Nanofibers and their applications in tissue engineering. *Int. J. Nanomed.* **2006**, *1*, 15–30. [[CrossRef](#)] [[PubMed](#)]
6. Nogi, M.; Yano, H. Transparent nanocomposites based on cellulose produced by bacteria offer potential innovation in the electronics device industry. *Adv. Mater.* **2008**, *20*, 1849–1852. [[CrossRef](#)]
7. Abdul Khalil, H.P.S.; Davoudpour, Y.; Saurabh, C.K.; Hossain, M.S.; Adnan, A.S.; Dungani, R.; Paridah, M.T.; Mohamed, Z.I.S.; Fazita, M.R.N.; Syakir, M.I.; et al. A review on nanocellulosic fibres as new material for sustainable packaging: Process and applications. *Renew. Sustain. Energy Rev.* **2016**, *64*, 823–836. [[CrossRef](#)]
8. Ifuku, S. Chitin nanofibers: Preparations, modifications, and applications. In *Handbook Polymer Nanocomposites. Processing, Performance and Application*; Pandey, J.K., Takagi, H., Nakagaito, A.N., Kim, H.-J., Eds.; Springer: Berlin/Heidelberg, Germany, 2015; Volume C: Polymer Nanocomposites Cellulose Nanoparticles, pp. 165–178.
9. Food and Agriculture Organization of the United Nations. *The State of World Fisheries and Aquaculture—Meeting the Sustainable Development Goals*; Food and Agriculture Organization of the United Nations: Rome, Italy, 2018.
10. Lopes, C.; Antelo, L.T.; Franco-Uría, A.; Alonso, A.A.; Pérez-Martín, R. Chitin production from crustacean biomass: Sustainability assessment of chemical and enzymatic processes. *J. Clean. Prod.* **2018**, *172*, 4140–4151. [[CrossRef](#)]
11. Sagheer, F.A.A.; Al-Sughayer, M.A.; Muslim, S.; Elsabee, M.Z. Extraction and characterization of chitin and chitosan from marine sources in Arabian Gulf. *Carbohydr. Polym.* **2009**, *77*, 410–419. [[CrossRef](#)]
12. Arbia, W.; Arbia, L.; Adour, L.; Amrane, A. Chitin extraction from crustacean shells using biological methods—A review. *Food Technol. Biotechnol.* **2013**, *51*, 12–25.

13. Yang, H.; Gözaydın, G.; Nasaruddin, R.R.; Har, J.R.G.; Chen, X.; Wang, X.; Yan, N. Towards the shell biorefinery: Processing crustacean shell waste using hot water and carbonic acid. *ACS Sustain. Chem. Eng.* **2019**, *7*, 5532–5542. [[CrossRef](#)]
14. Nilsen-Nygaard, J.; Strand, S.P.; Vårum, K.M.; Draget, K.I.; Nordgård, C.T. Chitosan: Gels and interfacial properties. *Polymers* **2015**, *7*, 552–579. [[CrossRef](#)]
15. Zhang, X.; Rolandi, M. Engineering strategies for chitin nanofibers. *J. Mater. Chem. B* **2017**, *5*, 2547–2559. [[CrossRef](#)] [[PubMed](#)]
16. Jayakumar, R.; Prabakaran, M.; Nair, S.V.; Tamura, H. Novel chitin and chitosan nanofibers in biomedical applications. *Biotechnol. Adv.* **2017**, *28*, 142–150. [[CrossRef](#)] [[PubMed](#)]
17. Ifuku, S.; Nogi, M.; Yoshioka, M.; Morimoto, M.; Yano, H.; Saimoto, H. Fibrillation of dried chitin into 10–20 nm nanofibers by a simple grinding method under acidic conditions. *Carbohydr. Polym.* **2010**, *81*, 134–139. [[CrossRef](#)]
18. Hassan, M.L.; Hassan, E.; Oksman, K.N. Effect of pretreatment of bagasse fibers on the properties of chitosan/microfibrillated cellulose nanocomposites. *J. Mater. Sci.* **2011**, *46*, 1732–1740. [[CrossRef](#)]
19. Azeredo, H.M.C.; Mattoso, L.H.C.; Avena-Bustillos, R.J.; Filho, G.C.; Munford, M.L.; Wood, D.; McHugh, T.H. Nanocellulose reinforced chitosan composite films as affected by nanofiller loading and plasticizer content. *J. Food Sci.* **2010**, *75*, N1–N7. [[CrossRef](#)] [[PubMed](#)]
20. Maevskaia, E.N.; Shabunin, A.S.; Dresvyanina, E.N.; Dobrovol'skaya, I.P.; Yudin, V.E.; Paneyah, M.B.; Fediuk, A.M.; Sushchinskii, P.L.; Smirnov, G.P.; Zinoviev, E.V.; et al. Influence of the introduced chitin nanofibrils on biomedical properties of chitosan-based materials. *Nanomaterials* **2020**, *10*, 945. [[CrossRef](#)] [[PubMed](#)]
21. Okamoto, Y.; Yano, R.; Miyatake, K.; Tomohiro, I.; Shigemasa, Y.; Minami, S. Effects of chitin and chitosan on blood coagulation. *Carbohydr. Polym.* **2003**, *53*, 337–342. [[CrossRef](#)]
22. de Lima, J.M.; Sarmiento, R.R.; de Souza, J.R.; Brayner, F.A.; Feitosa, A.P.S.; Padilha, R.; Alves, L.C.; Porto, I.J.; Batista, R.F.B.D.; de Oliveira, J.E.; et al. Evaluation of hemagglutination activity of chitosan nanoparticles using human erythrocytes. *BioMedical Res. Int.* **2015**, *2015*, 247965.
23. Klokkeuold, P.R.; Fukayama, H.; Sung, E.C.; Bertolami, C.N. The effect of chitosan (poly-N-acetylglucosamine) on lingual hemostasis in heparinized rabbits. *J. Oral Maxillofac. Surg.* **1999**, *57*, 49–52. [[CrossRef](#)]
24. Millner, R.; Lockhart, A.S.; Marr, R. Chitosan arrests bleeding in major hepatic injuries with clotting dysfunction: An in vivo experimental study in a model of hepatic injury in the presence of moderate systemic heparinisation. *Ann. R. Coll. Surg. Engl.* **2010**, *92*, 559–561. [[CrossRef](#)]
25. Dai, T.; Tanaka, M.; Huang, Y.Y.; Hamblin, M.R. Chitosan preparations for wounds and burns: Antimicrobial and wound-healing effects. *Expert Rev. Anti Infect. Ther.* **2011**, *9*, 857–879. [[CrossRef](#)] [[PubMed](#)]
26. Jayakumar, R.; Prabakaran, M.; Sudheesh Kumar, P.T.; Nair, S.V.; Tamura, H. Biomaterials based on chitin and chitosan in wound dressing applications. *Biotechnol. Adv.* **2011**, *29*, 322–337. [[CrossRef](#)] [[PubMed](#)]
27. Brown, M.A.; Daya, M.R.; Worley, J.A. Experience with chitosan dressings in a civilian EMS system. *J. Emerg. Med.* **2009**, *37*, 1–7. [[CrossRef](#)] [[PubMed](#)]
28. Mlekusch, W.; Dick, P.; Haumer, M.; Sabeti, S.; Minar, E.; Schillinger, M. Arterial puncture site management after percutaneous transluminal procedures using a hemostatic wound dressing (Clo-Sur P.A.D.) versus onventional manual compression: A randomized controlled trial. *J. Endovasc. Ther.* **2006**, *13*, 23–31. [[CrossRef](#)] [[PubMed](#)]
29. Nguyen, N.; Hasan, S.; Caufield, L.; Ling, F.S.; Narins, C.R. Randomized controlled trial of topical hemostasis pad use for achieving vascular hemostasis following percutaneous coronary intervention. *Catheter. Cardiovasc. Intervals* **2007**, *69*, 801–807. [[CrossRef](#)] [[PubMed](#)]
30. Littlejohn, L.; Bennett, B.L.; Drew, B. Application of current hemorrhage control techniques for backcountry care: Part two, hemostatic dressings and other adjuncts. *Wilderness Environ. Med.* **2015**, *26*, 246–254. [[CrossRef](#)] [[PubMed](#)]
31. Percot, A.; Viton, C.; Domard, A. Characterization of shrimp shell deproteinization. *Biomacromolecules* **2003**, *4*, 1380–1385. [[CrossRef](#)] [[PubMed](#)]
32. Percot, A.; Viton, C.; Domard, A. Optimization of chitin extraction from shrimp shells. *Biomacromolecules* **2002**, *4*, 12–18. [[CrossRef](#)]
33. Aklog, Y.F.; Egusa, M.; Kaminaka, H.; Izawa, H.; Morimoto, M.; Saimoto, H.; Ifuku, S. Protein/CaCO₃/Chitin nanofiber complex prepared from crustacean shells by simple mechanical treatment and its effect on plant growth. *Int. J. Mol. Sci.* **2016**, *17*, 1600. [[CrossRef](#)] [[PubMed](#)]
34. Tynngård, N.; Lindahl, T.L.; Ramström, S. Assays of different aspects of haemostasis—What do they measure? *Thromb. J.* **2015**, *13*, 8. [[CrossRef](#)]
35. Udvardi, B.; Kovács, I.J.; Fancsik, T.; Kónya, P.; Bátori, M.; Stercel, F.; Falus, G.; Szalai, Z. Effects of particle size on the attenuated total reflection spectrum of minerals. *Appl. Spectrosc.* **2017**, *71*, 1157–1168. [[CrossRef](#)] [[PubMed](#)]
36. Farmer, V.C.; Russell, J.D. Effects of particle size and structure on the vibrational frequencies of layer silicates. *Spectrochim. Acta* **1966**, *22*, 389–398. [[CrossRef](#)]
37. Jeon, C. Adsorption characteristics of waste crustacean shells for silver ions in industrial wastewater. *Korean J. Chem. Eng.* **2014**, *31*, 446–451. [[CrossRef](#)]
38. Pavia, D.L.; Lampman, G.M.; Kriz, G.S.; Vyvyan, J.A. *Introduction to Spectroscopy*; Cengage Learning: Boston, MA, USA, 2014.
39. Cárdenas, G.; Cabrera, G.; Taboada, E.; Miranda, S.P. Chitin characterization by SEM, FTIR, XRD, and ¹³C cross polarization/mass angle spinning NMR. *J. Appl. Polym. Sci.* **2004**, *93*, 1876–1885. [[CrossRef](#)]
40. Ioelovich, M. Crystallinity and hydrophilicity of chitin and chitosan. *J. Chem.* **2014**, *3*, 7–14.

41. Mogilevskaya, E.L.; Akopova, T.A.; Zelenetskii, A.N.; Ozerin, A.N. The crystal structure of chitin and chitosan. *Polym. Sci. Ser. A* **2006**, *48*, 116–123. [[CrossRef](#)]
42. Lavoine, N.; Bergström, L. Nanocellulose-based foams and aerogels: Processing, properties, and applications. *J. Mater. Chem. A* **2017**, *5*, 16105–16117. [[CrossRef](#)]
43. Gordeyeva, K.S.; Fall, A.B.; Hall, S.; Wicklein, B.; Bergström, L. Stabilizing nanocellulose-nonionic surfactant composite foams by delayed Ca-induced gelation. *J. Colloid Interface Sci.* **2016**, *472*, 44–51. [[CrossRef](#)] [[PubMed](#)]
44. Whang, H.S.; Kirsch, W.; Zhu, Y.H.; Yang, C.Z.; Hudson, S.M. Hemostatic agents derived from chitin and chitosan. *J. Macromol. Sci. Polym. Rev.* **2005**, *45*, 309–323. [[CrossRef](#)]
45. Ratner, B.D. The blood compatibility catastrophe. *J. Biomed. Mater. Res.* **1993**, *27*, 283–287. [[CrossRef](#)] [[PubMed](#)]
46. Karsa, D.R.; Stephenson, R.A. *Chemical Aspects of Drug Delivery Systems*; Royal Society of Chemistry: London, UK, 2007.
47. Bristow, S.M.; Gamble, G.D.; Stewart, A.; Horne, A.M.; Reid, I.R. Acute effects of calcium supplements on blood pressure and blood coagulation: Secondary analysis of a randomised controlled trial in post-menopausal women. *J. Nutr.* **2015**, *114*, 1868–1874. [[CrossRef](#)]
48. Hilgard, P. Experimental hypercalcaemia and whole blood clotting. *J. Clin. Pathol.* **1973**, *26*, 616–619. [[CrossRef](#)]
49. Vines, H. *The Coagulation of the Blood. Part I. The Role of Calcium*; Springer: New York, NY, USA, 2014.